



# Interface Control of Emergent Ferroic Order in Ruddlesden-Popper $\text{Sr}_{n+1}\text{Ti}_n\text{O}_{3n+1}$

Turan Birol, Nicole A. Benedek, and Craig J. Fennie

*School of Applied Engineering Physics, Cornell University, Ithaca, New York 14853, USA*  
(Received 7 October 2011; published 13 December 2011; corrected 27 December 2011)

We discovered from first principles an unusual polar state in the low  $n$   $\text{Sr}_{n+1}\text{Ti}_n\text{O}_{3n+1}$  Ruddlesden-Popper (RP) layered perovskites in which ferroelectricity is nearly degenerate with antiferroelectricity, a relatively rare form of ferroic order. We show that epitaxial strain plays a key role in tuning the “perpendicular coherence length” of the ferroelectric mode, and does not induce ferroelectricity in these low-dimensional RP materials as is well known to occur in  $\text{SrTiO}_3$ . These systems present an opportunity to manipulate the coherence length of a ferroic distortion in a controlled way, without disorder or a free surface.

DOI: 10.1103/PhysRevLett.107.257602

PACS numbers: 77.84.-s, 77.80.-e

Control over the emergence of (anti)ferroelectric and antiferrodistortive order remains a fundamental challenge for the atomic-scale rational design of new phenomena. Complex oxide heterostructures, layered thin films, and other low-dimensional systems provide a novel platform to address this ongoing challenge. There have been two well-explored approaches to control ferroicity in these systems: epitaxial strain engineering—which has been used to induce ferroelectricity [1], multiferroicity [2], and to create strongly coupled multiferroics [3]—and tailoring electrostatic boundary conditions. A significant challenge in the field of ferroelectric thin films has been understanding the evolution of the spontaneous polarization ( $P_{\perp}$  in Fig. 1) in ferroelectric-paraelectric heterostructures [4] and ferroelectric nanoscale thin film capacitors as the dimension parallel to the polarization direction is reduced [5–9]. Today it is clear that this is driven almost entirely by the electrostatic depolarizing field arising at the interface.

(Anti)Ferroelectric and antiferrodistortive distortions are cooperative phenomena involving the coherent motion of atoms extending over many unit cells [10]. Therefore, these ferroic states may also be greatly influenced by introducing a perturbation with a characteristic length scale below (or near) that of the coherence length of the ferroic distortion [11,12]. Design strategies based on such an effect have lead to the emergence of many novel ferroic states, such as multiferroicity [13] and relaxor ferroelectricity. The ability to control ferroic order on the scale of the coherence length therefore represents an opportunity to understand and create novel ferroic phenomena. However, in bulk materials, the only known tuning mechanisms are atomic disorder (which in many cases tends to introduce electronic defects that are detrimental to the desired properties) or free surfaces [14]. Clearly, alternative pathways are desired.

In this Letter we show how a complex oxide interface can exploit the coherence length of a ferroic instability in a controlled way and use it to design an unusual polar state

in which ferroelectricity is nearly degenerate with antiferroelectricity, a relatively rare form of ferroic order. In contrast to the well-studied “finite-size effects” problem in (anti)ferroelectrics [15], the physics discussed here involves the emergence of local polar instabilities in a direction parallel to the interface. For such an in-plane direction, the polarization ( $P_{\parallel}$  in Fig. 1) never comes “in contact” with the interface, electrostatic boundary conditions correspond to a short circuit, perfect screening of the depolarization field is always achieved, and the system is structurally infinite.

As a model system we take the perovskite-rocksalt interface in the naturally occurring Ruddlesden-Popper (RP) layered perovskite,  $\text{Sr}_{n+1}\text{Ti}_n\text{O}_{3n+1}$ . Dielectric studies and previous first-principles calculations have shown that

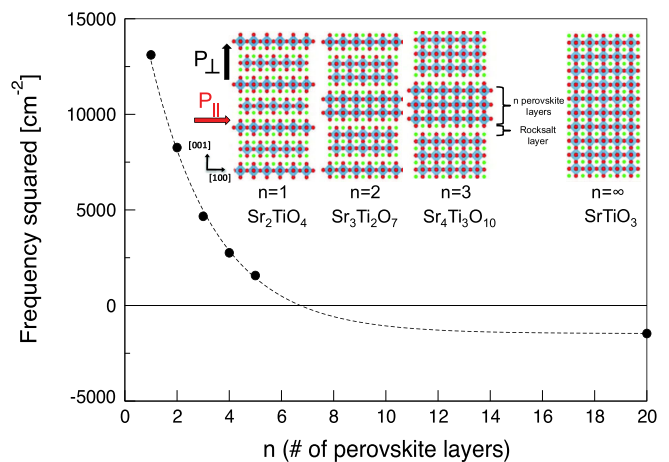


FIG. 1 (color online). (Inset) The Ruddlesden-Popper,  $\text{Sr}_{n+1}\text{Ti}_n\text{O}_{3n+1}$ , homologous series showing two possible polarization directions: in-plane,  $P_{\parallel}$ , and out-of-plane,  $P_{\perp}$ . (Main figure) Calculated in-plane polar phonon frequency as a function of  $n$  for a fixed in-plane lattice constant of  $\text{SrTiO}_3$ . (The dots are first-principles calculations; the curve is a fit to a single exponential.)

low- $n$  members of the series ( $n = 1-5$ ) are paraelectric with low dielectric permittivities [16,17]. This is surprising given that the structure of the RP homologous series [18,19], alternatively written as  $(\text{SrTiO}_3)_n/(\text{SrO})$ , can be thought of as a  $\text{SrTiO}_3$  perovskite with an extra SrO monolayer inserted every  $n$  perovskite unit cells along [001] as shown in the inset of Fig. 1.  $\text{SrTiO}_3$  (the  $n = \infty$  member of the RP series) is a well-known quantum paraelectric (QP) that displays a large dielectric constant ( $\approx 10\,000$  at low temperature) and can be driven ferroelectric with the application of a modest amount of biaxial strain [1,20].

The key discovery we make is that structural relaxations occurring at the RP fault, that is, at the SrO/SrTiO<sub>3</sub> interface, break the coherence of the infinitely long Ti-O-Ti chains parallel to the interface in different perovskite slabs. Even at a tensile strain value more than sufficient to drive  $\text{SrTiO}_3$  ferroelectric (where the polarization lies in plane,  $P_{\parallel}$ ), here we find that the  $n = 1$  RP is still very far from displaying a polar instability, even though the electrical boundary conditions and the length of the Ti-O-Ti chains in the relevant direction are identical to that of  $\text{SrTiO}_3$ . An in-plane polar state must emerge with increasing  $n$ , the nature of which and how or why this happens is unknown. In the remainder of this Letter we explore these questions and show how, unlike in  $\text{SrTiO}_3$ , epitaxial strain does not induce ferroelectricity in these materials. Instead, we elucidate the novel role of strain in tuning the perpendicular coherence length of the polar mode and use it to tune a system to a region of the phase diagram where ferroelectricity and antiferroelectricity compete with each other.

We performed density-functional theory (DFT) calculations within the PBEsol approximation using PAW potentials, as implemented in VASP [21–24]. The wave functions were expanded in plane waves up to a cutoff of 500 eV. Integrals over the Brillouin zone were approximated by sums on a  $\Gamma$ -centered  $k$ -point mesh consistent with an  $8 \times 8 \times 8$  mesh for the primitive perovskite unit cell. A low force threshold of 0.5 meV/Å was used for all geometric relaxations in order to resolve the small energy differences. Phonon frequencies and eigendisplacements were calculated using two methods: the direct method using symmetry adapted modes in VASP and density-functional perturbation theory (DFPT) as implemented in the QUANTUM ESPRESSO package. For the DFPT calculations, Vanderbilt ultrasoft pseudopotentials were used within local density approximation. We ignore quantum fluctuations of nuclei and therefore bulk  $\text{SrTiO}_3$  is predicted to have a ferroelectric ground state (see Supplemental Material [25]).

To begin to unravel the novel polar state that emerges in strained RP phases, we calculate the in-plane polar ( $E_u$ ) phonon frequencies of the  $n = 1$  to  $n = 5$  members and the  $n = \infty$  bulk. We fix the in-plane lattice constant of all RP structures to that of theoretical  $\text{SrTiO}_3$ ,  $a = 3.899$  Å.

Note that the equilibrium in-plane lattice constant  $a$  increases monotonically with increasing  $n$ ; the  $n = 1$  member,  $\text{Sr}_2\text{TiO}_4$ , has a 0.5% smaller lattice constant than bulk perovskite  $\text{SrTiO}_3$ . As Fig. 1 shows, the soft mode frequency decreases monotonically with increasing  $n$ , even though the in-plane lattice constant was fixed to the same value for all  $n$  (and therefore the in-plane strain is actually decreasing with increasing  $n$ ). Such a trend is surprising. The observed decay of the phonon frequency with increasing  $n$  can in fact be easily modeled. It is exactly what one would find in a toy model calculation of the interplanar force constants of a finite thick, infinite slab as more layers are added to the slab (see Supplemental Material [25]). It is, however, not clear why the RP phases, which are bulk materials, should display this kind of crossover from two-dimensional to three-dimensional behavior as  $n$  increases, given that the Ti-O-Ti chains are continuous and infinite parallel to the direction of the polar mode. Additionally, why does the polar mode of the  $n = 1$  member have such a high frequency? We propose that in  $\text{SrTiO}_3$  there is a coherence length perpendicular to the direction of the polar mode and that coherence between different perovskite blocks is broken by the double rocksalt layers in the RP phases, effectively reducing the dimensionality of the system. There are therefore two questions that need to be answered: (1) does it make sense that a perpendicular coherence length exists in  $\text{SrTiO}_3$  and if so can it be manipulated? and (2) can the double rocksalt layer really suppress the coherence between perovskite blocks?

*Critical thickness.*—Our basic premise is that the real-space coherence requirements of the lattice instabilities in the RP phases can be deduced from the phonon dispersion curves of the bulk cubic perovskite. Figure 2(a) shows that there are two main instabilities for bulk  $\text{SrTiO}_3$ : an  $R$ -point instability involving rotations of the oxygen octahedra, and the unstable polar mode at  $\Gamma$ . An alternative way to visualize the distribution of lattice instabilities in reciprocal space is by plotting the  $\omega^2 = 0$  isosurface in the first Brillouin zone [12,26], Fig. 2(b). The enclosed volumes on the zone boundary correspond to the  $R$ -point octahedral rotation instability and the FE instability is associated with the volume in the zone center. We point out that this picture is similar to that obtained by Lasota *et al.* [27], who previously considered the coherence properties of the  $R$ -point rotation instability only. Figure 2(a) shows that the branch stemming from the  $\Gamma$  instability becomes stable at wave vectors away from  $\Gamma$  in all the of high symmetry directions—towards  $X$ ,  $M$ , or  $R$ —and is therefore localized in reciprocal space to a finite volume around the zone center.

From Fig. 2(b) it is seen that the volume of the FE instability has a strongly anisotropic structure: it consists of three perpendicular disks. Each disk encloses wave vectors that have an instability involving ionic displacements in the direction perpendicular to the plane

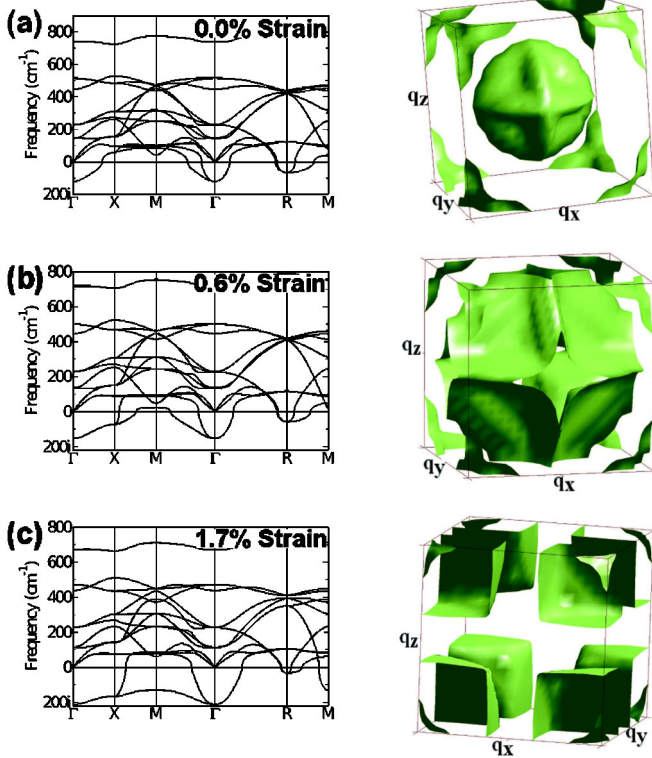


FIG. 2 (color online). Phonon dispersions of SrTiO<sub>3</sub> in its cubic ( $Pm\bar{3}m$ ) phase at (a) experimental volume, and under (b) 0.6% and (c) 1.7% isotropic tensile strain with respect to the experimental lattice constant. The corresponding  $\omega^2 = 0$  isosurfaces are shown next to each phonon dispersion curve.

of the disk. The finite thickness of the disks, corresponding to a finite longitudinal coherence length,  $l_{\parallel} \sim 1/q_{\parallel}$ , has been previously discussed in perovskite ferroelectrics such as BaTiO<sub>3</sub> [12] and KNbO<sub>3</sub> [26]. The finite radius of the unstable disks in the reciprocal space found in SrTiO<sub>3</sub> suggests that the frequency of the unstable branch also depends on the perpendicular component of the wave vector, corresponding to a finite perpendicular coherence length,  $l_{\perp} \sim 1/q_{\perp}$  (see Supplemental Material [25]). In contrast, in BaTiO<sub>3</sub> [12] and KNbO<sub>3</sub> [26] the isosurfaces consist of three almost perfectly flat slabs that are infinitely extended, indicating that the frequency of the unstable branch is the same regardless of the component of the wave vector that is perpendicular to the direction of the ionic displacements. This implies that the critical thickness for an infinite slab of BaTiO<sub>3</sub> is zero [28].

Assuming the rocksalt layers break the perpendicular coherence between different perovskite blocks (we will shortly prove this is true), the nonvanishing critical thickness required for ferroelectricity in SrTiO<sub>3</sub> imposes a geometric condition,  $n_{\text{crit}}$ , for RPs to display an in-plane ferroelectric instability;  $n < n_{\text{crit}}$  members cannot have an energy lowering FE distortion simply because the number

of perovskite blocks between the rocksalt layers do not satisfy the coherence condition. However, as  $n$  increases, the structures should get closer to the FE transition. This is exactly what we have shown in Fig. 1, where the soft mode frequency  $\omega$  vanishes at  $n_{\text{crit}} \sim 7$ , agreeing with the lower bound from the reciprocal space picture of the instability of SrTiO<sub>3</sub>.

*Tuning the coherence length.*—The effects of strain [29] and pressure [30] on ferroelectricity in perovskites are well known; they alter the balance between the short-range forces (which favor the centrosymmetric state) and long-range Coulomb forces (which favor the ferroelectric state). But what are their effects on the coherence requirements? In Figs. 2(b) and 2(c) we plot the phonon dispersion curves and the corresponding  $\omega^2 = 0$  isosurfaces of cubic SrTiO<sub>3</sub> for isotropic tensile strains of 0.6% and 1.7%, respectively. As shown, negative pressure not only softens the  $\Gamma$  instability (the well-known strain-induced ferroelectricity [20]) but also increases the volume of unstable  $q$  vectors in

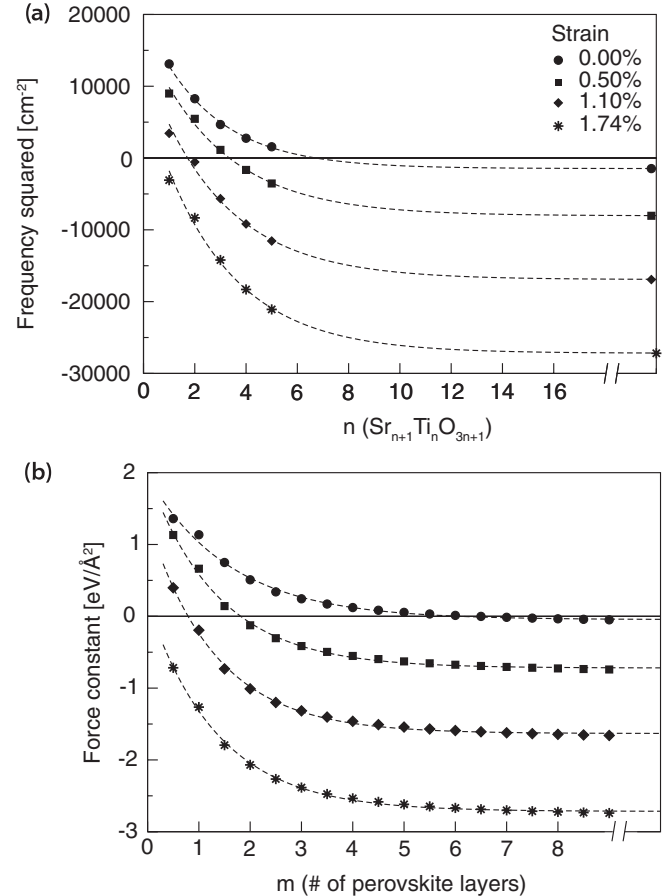


FIG. 3. (a) Ruddlesden-Popper,  $(\text{SrTiO}_3)_n(\text{SrO})$ : in-plane polar soft mode frequency squared versus layering number  $n$ . (b) Perovskite slab model,  $(\text{SrTiO}_3)_m$ : lowest in-plane polar interplanar force constant matrix eigenvalue versus thickness of SrTiO<sub>3</sub>. Strain values are given with respect to the lattice constant of SrTiO<sub>3</sub>. The lines are fits to exponentials.

reciprocal space. By 0.6% strain, the instability reaches the  $X$  point and at 1.7% strain the branch is unstable and relatively dispersionless in the entire  $\Gamma$ - $X$ - $M$  plane. In fact, the  $\omega^2 = 0$  isosurface at this isotropic strain value resembles that of  $\text{BaTiO}_3$  [12].

These results suggest that under increasing biaxial, in-plane tensile strain [31] the critical thickness for in-plane ferroelectricity in  $\text{SrTiO}_3$ , and hence  $n_{\text{crit}}$  in the RPs, should decrease and eventually vanish. This is clearly seen for the RPs in Fig. 3(a). Note that at a tensile strain value of 1.1%—a strain more than sufficient to drive  $\text{SrTiO}_3$  ferroelectric—the perpendicular coherence length ( $l_{\perp}$ ) in  $\text{SrTiO}_3$  is still nonzero. This results in the  $n = 1$  RP remaining very far from displaying a polar instability. It is not until a strain of  $\sim 1.4\%$  that  $l_{\perp} \approx 0$  and the  $n = 1$  structure develops a polar instability.

As further proof of a crossover from 2D to 3D ferroelectric behavior (and the direct strain control thereof), we parametrize from first principles a finite thick, infinite perovskite slab force constant model for which we add additional layers of SrO and  $\text{TiO}_2$  planes. (For details, see Supplemental Material [25].) The softest force constant eigenvalue is plotted in Fig. 3(b) for different strain values as the number of  $\text{SrTiO}_3$  layers  $m$  is increased. Notice that the in-plane polar force constant in this 2D model slab [Fig. 3(b)] is evolving with both thickness and strain exactly like the in-plane polar instabilities in the structurally 3D RPs [Fig. 3(a)]. This is clear evidence of the proposed coherence physics and the direct control of with strain. (A similar calculation for unstrained  $\text{BaTiO}_3$ , which has a  $l_{\perp} \approx 0$ , shows that a single  $\text{TiO}_2$  layer in bulk  $\text{BaTiO}_3$  is unstable.)

*The effects of rumpling.*—These results suggest that the rocksalt layer in  $\text{Sr}_{n+1}\text{Ti}_n\text{O}_{3n+1}$  breaks the coherence between perovskite blocks. Why and how does this happen? Note that rumpling of the SrO layers is permitted by symmetry in paraelectric RPs and that the distance along the [001] direction between the Sr and O ions within the rocksalt layer can be as large as 0.20 Å [32] and quickly gets smaller in the layers farther away, Fig. 4(b). In RPs with  $n > n_{\text{crit}}$ , the in-plane polar displacements of Ti along the infinite Ti-O-Ti chains get smaller the closer the chain is to the rocksalt layer. We propose that the rumpling at the double SrO layers breaks the coherence between perovskite slabs.

To test this hypothesis, we artificially zero the rumpling by moving the Sr and Ti atoms to exactly the same plane as the oxygens, and repeat the phonon calculations. We find that even the  $n = 1$   $\text{Sr}_2\text{TiO}_4$  under zero strain has an in-plane polar instability and it is in fact almost equal in magnitude to that of  $\text{SrTiO}_3$ , that is, the decay of the phonon frequency with  $n$  disappears [33].

What are the implications of our findings? We propose that strained RPs, which lack coherence across the rocksalt layers, cannot be ferroelectric, but rather display a novel

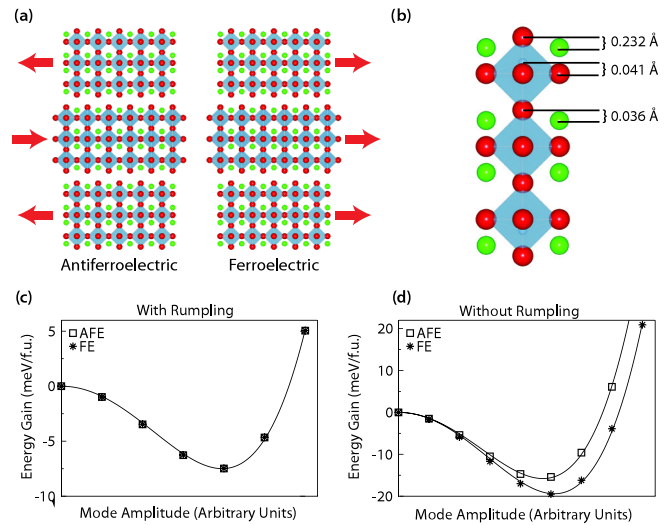


FIG. 4 (color online).  $\text{Sr}_4\text{Ti}_3\text{O}_{10}$  ground state under 1.1% tensile strain. (a) Schematic of ferroelectric (FE) and antiferroelectric (AFE) distortions. (b) Rumpling distortion (defined as the distance along [001] between cations and oxygens on the same layer). (c) Energy gain due to FE and AFE distortions in structures with rumpling. (d) The same as (c) except the rumpling distortion has been artificially set to zero.

polar state. In Fig. 4(c) we plot the energy versus mode amplitude in, e.g.,  $\text{Sr}_4\text{Ti}_3\text{O}_7$  ( $n = 3$ ) for both the ferroelectric mode and an antiferroelectric distortion involving polar distortions of neighboring perovskite slabs antiparallel to each other [Fig. 4(a) shows a comparison of these modes]. Notice that the energy surfaces for these distortions are degenerate up to the precision of this plot. In Fig. 4(d) we plot the results of a similar calculation except that the rumpling was artificially zeroed; without rumpling, the degeneracy of the antiferroelectric (AFE) and FE modes is lifted. These calculations (we found similar results for  $n = 1, 2$ , and 3 at two different values of strain) prove that the RP fault indeed breaks the coherence between perovskite slabs, resulting not only in a suppression of polar distortions for  $n < n_{\text{crit}}$ , but also for  $n > n_{\text{crit}}$  polar distortions in neighboring perovskite slabs do not interact with each other significantly even at higher than quadratic order. All of this suggests that there are an infinite number of degenerate states involving uncorrelated atomic-scale polar regions. We surmise that the ground state may be a form of relaxor ferroelectricity without disorder, the consequences of which remain unclear.

The initial motivation for this project grew out of discussions between C. J. F. and D. G. Schlom. T. B. acknowledges useful discussions with David Vanderbilt at Ferro 2011. T. B. was supported by Penn State NSF-MRSEC Grant No. DMR 0820404. N. A. B. was supported by the Cornell Center for Materials Research with funding from the NSF-MRSEC program, cooperative agreement DMR 1120296. C. J. F. was supported by the NSF (No. DMR-1056441).

- [1] J. Haeni *et al.*, *Nature (London)* **430**, 758 (2004).
- [2] S. Bhattacharjee, E. Bousquet, and P. Ghosez, *Phys. Rev. Lett.* **102**, 117602 (2009).
- [3] C.J. Fennie and K.M. Rabe, *Phys. Rev. Lett.* **97**, 267602 (2006).
- [4] J.B. Neaton and K.M. Rabe, *Appl. Phys. Lett.* **82**, 1586 (2003).
- [5] I. Kornev, H. Fu, and L. Bellaiche, *Phys. Rev. Lett.* **93**, 196104 (2004).
- [6] J. Junquera and P. Ghosez, *Nature (London)* **422**, 506 (2003).
- [7] R. V. Wang *et al.*, *Phys. Rev. Lett.* **102**, 047601 (2009).
- [8] M. Stengel and N. A. Spaldin, *Nature (London)* **443**, 679 (2006).
- [9] N. Sai, A.M. Kolpak, and A.M. Rappe, *Phys. Rev. B* **72**, 020101 (2005).
- [10] M. Lines and A. Glass, *Principles and Applications of Ferroelectrics and Related Materials* (Clarendon Press, Oxford, 1977).
- [11] D.I. Bilc and D.J. Singh, *Phys. Rev. Lett.* **96**, 147602 (2006).
- [12] P.H. Ghosez, X. Gonze, and J.P. Michenaud, *Ferroelectrics* **206**, 205 (1998).
- [13] D.J. Singh and C.H. Park, *Phys. Rev. Lett.* **100**, 087601 (2008).
- [14] B. Meyer and D. Vanderbilt, *Phys. Rev. B* **63**, 205426 (2001).
- [15] E. Bousquet, J. Junquera, and P. Ghosez, *Phys. Rev. B* **82**, 045426 (2010).
- [16] J. H. Haeni, C. D. Theis, D. G. Schlom, W. Tian, X. Q. Pan, H. Chang, I. Takeuchi, and X.-D. Xiang, *Appl. Phys. Lett.* **78**, 3292 (2001).
- [17] N.D. Orloff *et al.*, *Appl. Phys. Lett.* **94**, 042908 (2009).
- [18] S.N. Ruddlesden and P. Popper, *Acta Crystallogr.* **10**, 538 (1957).
- [19] S.N. Ruddlesden and P. Popper, *Acta Crystallogr.* **11**, 54 (1958).
- [20] A. Antons, J.B. Neaton, K.M. Rabe, and D. Vanderbilt, *Phys. Rev. B* **71**, 024102 (2005).
- [21] G. Kresse and J. Hafner, *Phys. Rev. B* **47**, 558 (1993).
- [22] G. Kresse and J. Furthmüller, *Phys. Rev. B* **54**, 11 169 (1996).
- [23] P.E. Blöchl, *Phys. Rev. B* **50**, 17 953 (1994).
- [24] G. Kresse and D. Joubert, *Phys. Rev. B* **59**, 1758 (1999).
- [25] See Supplemental Material at <http://link.aps.org/supplemental/10.1103/PhysRevLett.107.257602> for a detailed discussion of the perpendicular coherence length, the interplanar force constants model, and also an estimate of the transition temperatures.
- [26] R. Yu and H. Krakauer, *Phys. Rev. Lett.* **74**, 4067 (1995).
- [27] C. Lasota, C.-Z. Wang, R. Yu, and H. Krakauer, *Ferroelectrics* **194**, 109 (1997).
- [28] G. Geneste, E. Bousquet, and P. Ghosez, *J. Comput. Theor. Nanosci.* **5**, 517 (2008) [<http://www.ingentaconnect.com/content/asp/jctn/2008/00000005/00000004/art00010>].
- [29] O. Diéguez, K.M. Rabe, and D. Vanderbilt, *Phys. Rev. B* **72**, 144101 (2005).
- [30] G.A. Samara, T. Sakudo, and K. Yoshimitsu, *Phys. Rev. Lett.* **35**, 1767 (1975).
- [31] D. Schlom, L.-Q. Chen, C.-B. Eom, K.M. Rabe, S.K. Streiffer, and J.-M. Triscone, *Annu. Rev. Mater. Res.* **37**, 589 (2007).
- [32] C.J. Fennie and K.M. Rabe, *Phys. Rev. B* **68**, 184111 (2003).
- [33] Note that strain has little influence on the amount of rumpling; rumpling does not differ by more than  $\sim 15\%$  in structures under different values of strain or with different  $n$ .